Geological characteristics and shale oil potential of the lacustrine immature to low mature shale oil system: a case study of the second member of Kongdian Formation in Cangdong Sag, Huanghua Depression, Bohai Bay Basin, China

Xiaoping Liu, Ming Guan, Zhijun Jin, Jin Lai & Shanyong Chen

Published online: 07 Oct 2020.

Submit your article to this journal

Article views: 126

View related articles

View Crossmark data

Taylor & Francis
Taylor & Francis Group

Check for updates

Geological characteristics and shale oil potential of the lacustrine immature to low mature shale oil system: a case study of the second member of Kongdian Formation in Cangdong Sag, Huanghua Depression, Bohai Bay Basin, China

Xiaoping Liu[a,b], Ming Guan [ID][a,b], Zhijun Jin[c,d], Jin Lai[a,b], and Shanyong Chen[e]

[a]State Key Laboratory of Petroleum Resources and Prospecting, China University of Petroleum (Beijing), Beijing, China; [b]College of Geosciences, China University of Petroleum (Beijing), Beijing, China; [c]State Key Laboratory of Shale Oil and Gas Enrichment Mechanisms and Effective Development, Beijing, China; [d]SINOPEC Petroleum Exploration and Production Research Institute, Beijing, China; [e]PetroChina Dagang Oil Field Company, Tianjing, China

ABSTRACT

The Second Member of Kongdian Formation (Ek_2) shale oil system is a set of thick organic-rich lacustrine shales with great shale oil resources potential. The shales are oil-prone with high organic matter abundance (samples with TOC > 2% accounting for 72.6%) and low maturity (the Ro of samples between 0.42% and 0.84%). The Ek_2 shale system is dominated by shales, sandstones, and carbonate rocks, which can be subdivided into various-mixed lithologies. The shales are primarily composed of clay minerals, quartz, feldspar, calcite, dolomite, pyrite, siderite, and zeolite, with no obvious predominant minerals. The brittle mineral content is high with an average content of 73.86%, which is conducive to reservoir stimulation. Physical properties and oil saturations vary significantly among different lithologies. Tight sandstones (average porosity 8.66%, average permeability 2.207×10^{-3} μm^2) and dolomites (average porosity 5.26%, average permeability 1.910×10^{-3} μm^2) have better exploration potential than shales (average porosity 2.46%, average permeability 0.937×10^{-3} μm^2). Considering Ro distribution, the slope zones are more favorable than Kongdian Structure Belt laterally and the lower intervals of the Ek_2 shale are more potential for shale oil accumulation than the upper interval vertically.

Introduction

The shale oil system is defined as a self-contained source-reservoir system, including organic-rich shale series and liquid hydrocarbons, where organic-rich shales or organic-lean intervals, e.g., sandstones and carbonate rocks, act as reservoirs (Jarvie 2012). The economic success of shale oil and gas in North America has inspired shale oil and gas exploration activities on other regions (Donovan et al. 2017; Jarvie 2012), whereas the geological characteristics and unconventional resources potential of lacustrine shales that can serve as the unconventional reservoirs are poorly understood. Unlike marine shales, the deposition of lacustrine shales was typically controlled by the paleoclimate, e.g., significant variation of lake levels due to climate change in a short geological period (thousands of years) limited the development of regional continuous thick shales and resulted in small-scale shale series in semi-deep to deep lakes. These shales are characterized by thin single layers but large accumulative thickness, which are frequently interbedded with sandstones and carbonate rocks (Katz and Lin 2014; Talbot 1988). Higher activation energy is required for hydrocarbon generation and crude oil

---

CONTACT Xiaoping Liu ✉ liuxiaoping@cup.edu.cn College of Geosciences, China University of Petroleum (Beijing), Beijing 102249, China

cracking in lacustrine shales, resulting in an oil window and gas window later than that of marine shales (Katz and Lin 2014; Tissot 1987).

Lacustrine organic-rich shales can be found in most Mesozoic-Cenozoic basins in China, in which immature to low-mature (Ro <0.7%) organic-rich shales are widely distributed (Huang and Li 1987; Wang et al. 1995). To date, conventional oil fields with liquid hydrocarbons from immature to low-mature source rocks have been found in several continental basins (Wang, Wei, and Zhao 2001; Zhou et al. 2002), which confirms the immense oil and gas resources potential of these lacustrine shales.

Oil exploration activities demonstrate that the second number of the Paleogene Kongdian Formation (Ek$_2$) in Cangdong Sag of the Bohai Bay Basin is a high-quality source layer, providing immature and low-mature oil for conventional reservoirs (Liu et al. 2015). Importantly, some active oil and gas shows and industrial oil flows from the Ek$_2$ indicate a considerable presence of immature to low-mature shale oil resources, and several wells obtained industrial oil production that exceeded 20 t/d, including Well GD6x1, KN9, etc. Ek$_2$ shales in oil-rich Cangdong Sag have been regarded as the key targets for the shale oil exploration (Zhao et al. 2018). The lithologies (Yan et al. 2017), geochemical characteristics (Liu et al. 2015), pore structures (Deng et al. 2020), and geological characteristics (Zhao et al. 2020, 2019) of the Ek$_2$ shales have been investigated preliminarily, but there is still a lack of understanding of the factors affecting shale oil accumulation, occurrence, and shale oil potential, which restricts the further shale oil exploration and exploitation. In this paper, the lithology, geochemistry, and reservoir qualities are integrated to expound the influence factors of shale oil system, evaluate the shale oil potential, and predict the favorable area of the Ek$_2$ shale in the Cangdong Sag, Huanghua Depression, Bohai Bay Basin. As a typical Cenozoic rift basin in eastern China, the study of immature to low-mature shale oil system in Cangdong Sag is of great significance for shale oil exploration in other basins with similar strata and evolution histories.

Geologic settings

The Cangdong Sag is a secondary structural unit of the Huanghua Depression, which spreads in the NE direction and controlled by the basin boundary faults. It is a Cenozoic intracontinental rift basin bounded by the Cangdong Fault to the northwest and the Xuhei Fault to the southwest with an exploration area of 4700 km^2 in the Paleogene (Zhao et al. 2018). The Cangdong Sag can be divided into five secondary structural units, i.e., the Kongdian Structural Belt, Eastern Kongdian Slope, Western Kongdian Slope, Nanpi Slope and Shenvshi Fault Nose (Figure 1). Through 40 years of exploration practices, seven conventional oil fields have been discovered. As the second largest oil-rich sag in Huanghua Depression, the Cangdong Sag is rich in oil and gas resources, with proven conventional crude oil reserves of 380 million tons and conventional natural gas reserves of 684 million cubic meters (Pu et al. 2016).

The Ek$_2$ was deposited in the rift stage by major deposition systems including braided river deltas, meandering river deltas, shallow lakes, and semi-deep to deep lakes (Figure 2) (Peng et al. 2010; Pu et al. 2016). It is dominated by black shales interbedded with thin siltstones or dolomites, where ferromagnesian intrusions can be found occasionally. The Ek$_2$ is distributed widely with thicknesses of 120 m ~ 600 m. It is regarded as a complete third-order sequence, which can be divided into four fourth-order sequences from bottom-to-top, including SQEk$_2^1$, SQEk$_2^2$, SQEk$_2^3$ and SQEk$_2^4$ (Pu et al. 2016). SQEk$_2^4$ is the low-stand system tract with delta front deposits composed of gray fine sandstone and gray mudstone assemblages. SQEk$_2^3$-SQEk$_2^2$ is the transgressive system tract, whose top is the maximum flooding surface of the Kongdian Formation. It is primarily a set of fine-grained deposits from semi-deep to deep lakes, mainly shale, argillaceous dolomite and siltstone, and gravity flow siltstone on the top. SQEk$_2^1$ is the high-stand system tract with the lower part dominated by dolomites and shales, and a set of shallow lacustrine mudstones deposited in the upper part (Figure 3). This paper focuses on the submembers of Ek$_2^1$, Ek$_2^2$ and Ek$_2^3$, while the Ek$_2^4$ submember mainly consists of conventional clastic reservoirs.
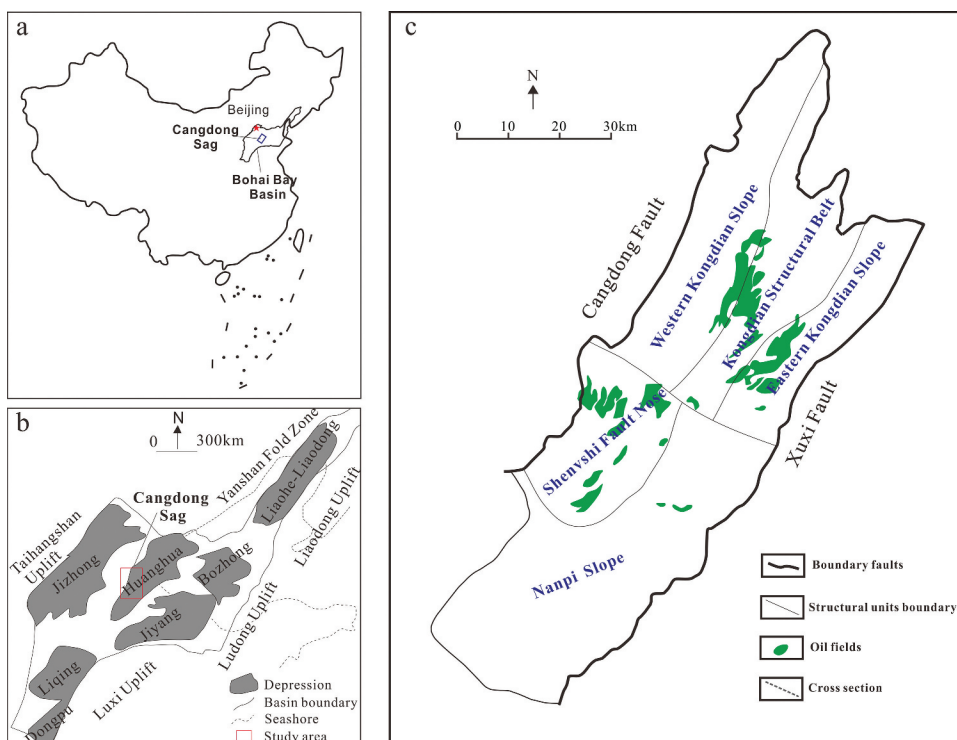
Figure 1. The location of the Cangdong Sag in China: (a) The location of Bohai Bay Basin; (b) The location of the study area; (c) the structural units and oil distributions in Cangdong Sag (Modified from Ye et al. (2013)).

Samples and methods

Twenty-nine samples were collected from 14 wells for a series of experiments, including total organic carbon content (TOC), chloroform bitumen "A," Rock-Eval pyrolysis, vitrinite reflectance (Ro), X-ray diffraction bulk rock, and clay mineral analysis (XRD), Ar-ion milling and field-emission scanning electron microscope (FE-SEM) observations, and pore structure analysis. TOC was measured using a LECOCS-200 carbon/sulfur analyzer. Chloroform bitumen "A" was obtained using the Soxhlet extraction method, the powered shale samples (<300 mesh) were extracted with chloroform/methanol (93:3) for 72 h to obtain the soluble organic matter. Rock-Eval pyrolysis was performed using a Vinci Rock-Eval 6 instrument to acquire the free hydrocarbon (S_1), the thermal cracking hydrocarbon (S_2), the peak temperature (Tmax) and the hydrocarbon index (HI). Ro values were determined using an MPV-III microphotometer as per the standard SY/T5124 (2012). The mineral composition was determined using a random-power XRD method by the Bruker D_2 PHASER X-ray diffraction, and the shale powder (<300 mesh) was placed in sample plate and was scanned from 4.5° to 50° with a step length 0.02°. The sections were produced, and petrographic information was analyzed using a polarizing light microscope. The 2D visualized analysis for the geometrical morphology and connectivity of the shale pores was completed by an FEI Quanta 200 F field-emission scanning electron microscope with an accelerating voltage of 20.0 kV and a working distance ranging from 9.0 mm to 11.0 mm. Pore structure characteristics were quantitatively determined by N_2 adsorption-desorption test using a TriStar II 3020 automatic specific surface area and pore volume analyzer, and the pore size distribution were calculated by BJH model (Barrett, Joyner, and Halenda 1951). All experiments were carried out at the China University of Petroleum (Beijing). In addition, some geochemical data were collected from the PetroChina Dagang Oilfield company.
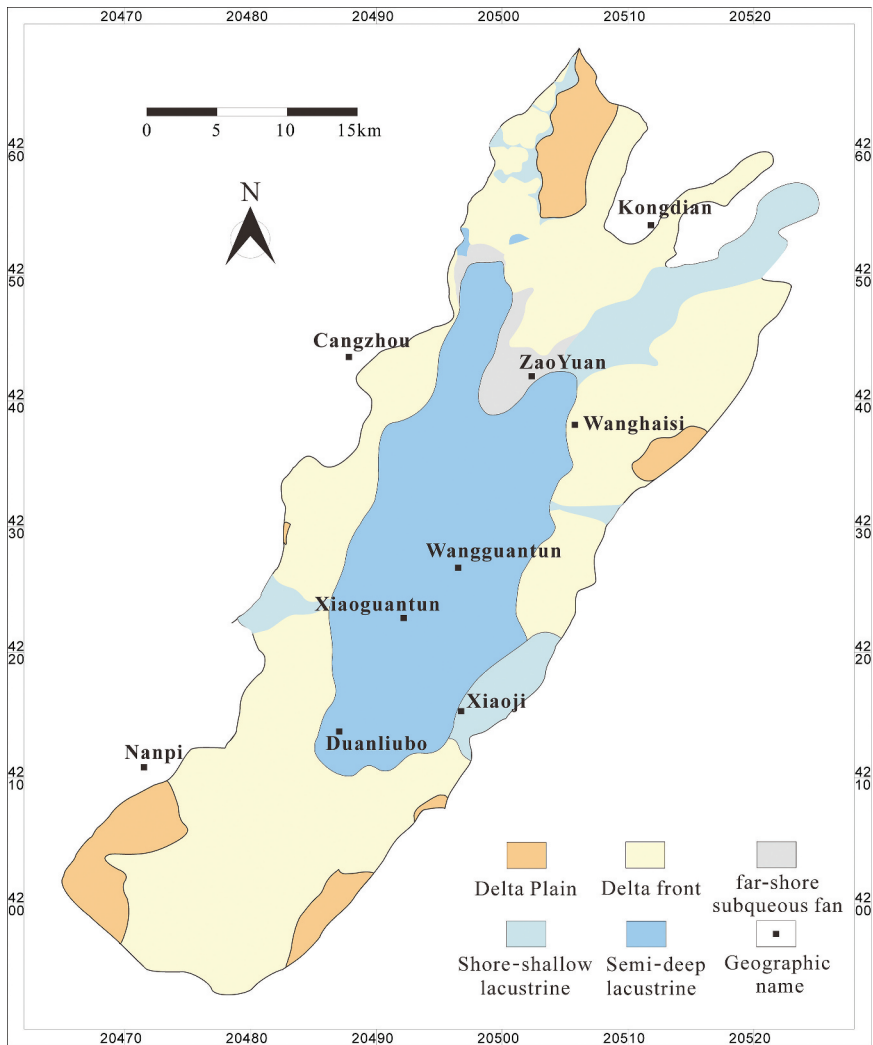
Figure 2. The sedimentary facies of the Ek$_2$ in the Cangdong Sag (Modified from Pu et al. (2016)).

Results

Lithology characteristics and mineralogy composition

Lithology characteristics

Core observation shows various lithologies in the Ek$_2$, indicating strong reservoir heterogeneity. Generally, three types of lithology can be found in cores, including shales, sandstones, and carbonate rocks, which are significantly different. Lithology variations can be observed from centimeter-scale core samples: gray or black shales (Figure 4a,d), dolomites (Figure 4b), and sandstones (Figure 4c).

A large number of thin-section observations indicate that the Ek$_2$ shale system has complex mineral compositions and multiple transitional facies. The three lithology types mentioned above can be subdivided into several subtypes. Specifically, shales include oil shale, mudstone, dolomitic shale, calcareous shale, and silty shale (Figure 5a–e). Oil shale is mainly composed of clay minerals with laminar structure, where organic matter can be found locally (Figure 5a). Mudstone is predominated by argillaceous components with minor sandy and carbonate components (Figure 5b). Silty shale is characterized by high sandy components (mainly quartz) with laminar structure, where siltstone is
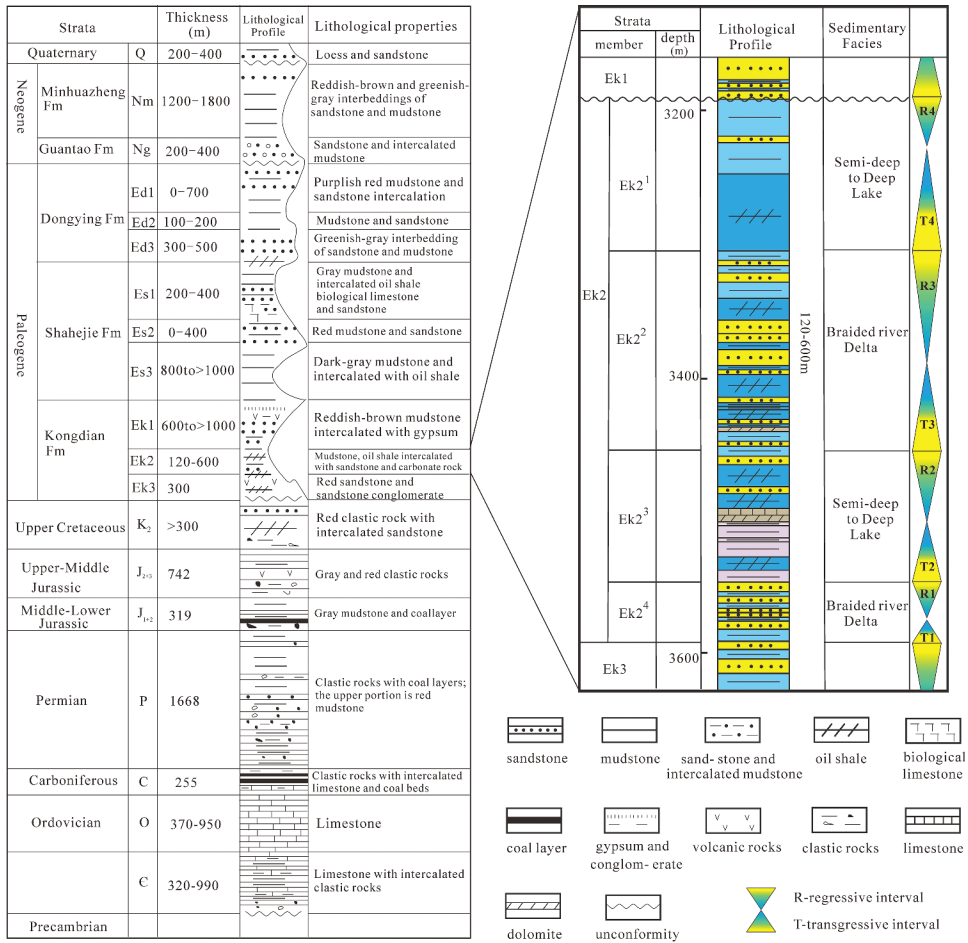
Figure 3. Stratigraphic columns of the Cangdong Sag and the Ek_2.

enriched in strips (Figure 5e). Dolomitic shale and calcareous shale are also laminar structures, which are dominated by clay minerals with certain dolomitic and calcareous components (Figure 5c ,d). Sandstone is commonly lithic siltstone, argillaceous sandstone, etc. (Figure 5f,g). Argillaceous siltstone is dominated by quartz and feldspar with certain content of clay and is partially contaminated by organic matter (Figure 5f). Lithic sandstone varies in grain size and has an obvious bedding structure, while the lithic debris mainly consists of sand debris and a small proportion of oolite (Figure 5g). Carbonate rocks are mainly dolomicrite, argillaceous dolomite, etc. (Figure 5h,i). Clay crystal structures are found in dolomites, indicating the occurrence of argillaceous components (Figure 5i).

Mineralogy composition

X-ray results suggest that the Ek_2 shale samples are primarily composed of clay minerals, quartz, feldspar, calcite, dolomite, analcime, pyrite, etc. (Table 1 and Figure 6). Clay mineral content varies between 3.2% and 67.2%, with an average value of 25.2%. Quartz and feldspar contents are in the ranges of 4.4%–55.9% and 1.2%–39.1%, with average values of 22.8% and 12.9%, respectively. Calcite and dolomite contents range from 0 to 21.9% and 0 to 82.6%, with average values of 6.4% and 18.7%, respectively. Analcime content varies between 0% and 38%, with an average value of 12.8%. In addition, there is minor pyrite and siderite (Table 1 and Figure 6). X-ray measurements agree well with core and thin-section observations, e.g., "shale" determined from the core are normally rich in clay minerals,
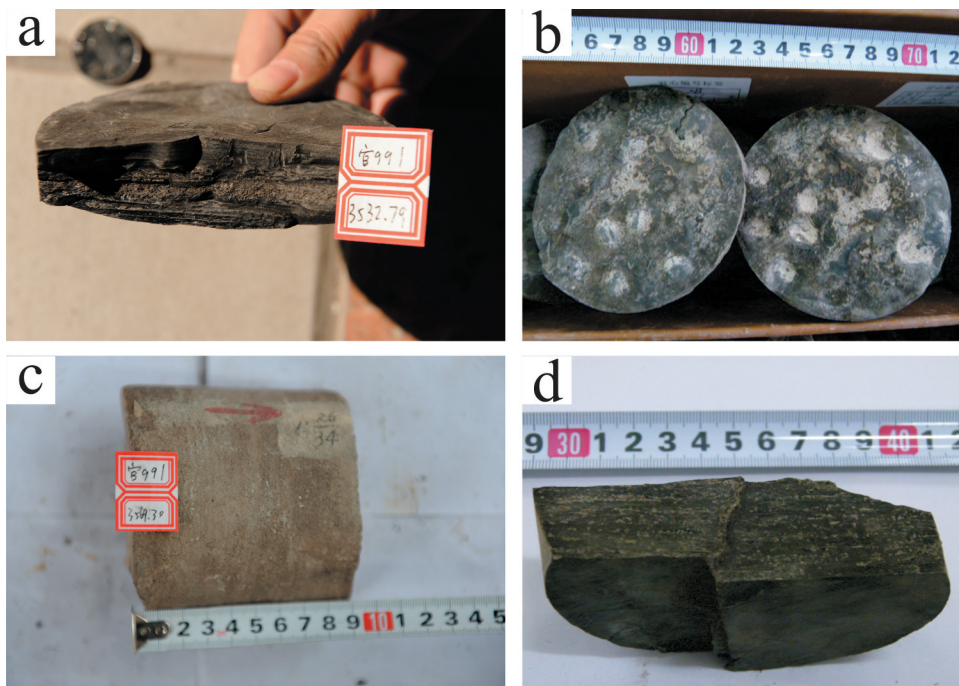
Figure 4. Core observations showing the lithologies in the Ek_2 shale system. (a) G991, 3532.79 m, dark gray oil shale, laminations; (b) F29-19, 2447.32 m, microcrystalline calcareous dolomite with oil tract in fractures, (c) G991, 3569.30 m, grayish-brown fine sandstone, (d) G995, 2890.73 m, gray-black dolomitic shale with dolomitic trip.

"sandstone" observed from the core had high quartz and feldspar content, and "dolomite" determined from the core is typically predominated by dolomite minerals (Figures 5 and 6).

The clay minerals are predominantly illite, kaolinite, chlorite, illite/smectite (I/S) and chlorite/smectite (C/S). I/S is also the most abundant mineral with a content up to 88% and an average value of 67.9%. Minor differences are noted among other clay minerals, e.g., illite has an average of 13% with a range of 6%–34%, kaolinite has an average of 4% with a range of 0–20%, chlorite has an average of 9% with a range of 2%–46%, chlorite/smectite has an average of 6% with a range of 0–45%, and the chlorite/smectite ratio has an average of 12% with a range of 0–45% (Table 1).

Organic geochemical characteristics

Organic matter abundance

Total organic carbon. Table 2 shows geochemical data from the study, and some geochemical data collected from the Dagang Oilfield are displayed in Table 3. The Ek_2^3 TOC is 0.04%–9.9%, averaging 3.44%; importantly, the samples with TOC more than 2% account for 72.6%. The Ek_2^2 TOC is 0.08%-7.43%, averaging 2.90%, and the samples with TOC more than 2% account for 64.8%. The Ek_2^1 TOC is 0.05%–9.40%, averaging 2.69%, while the samples with TOC more than 2% account for 48.7%. The average TOC of the Ek_2^2 and the Ek_2^3 are higher than that of the Ek_2^1 (Figure 7). The TOC distribution in the Ek_2^1, Ek_2^2 and Ek_2^3 were analyzed based on the measured TOC and the calculated TOC from well logs using the $\Delta logR$ model (Passey et al. 1990). The results show that the TOC distribution is obviously governed by sedimentary microfacies. Specifically, it is ring-like on the plane: the value is high in the deep to semi-deep lake in the center of the depression and decreases toward the boundary. In addition, the Ek_2^1, Ek_2^2 and Ek_2^3 are similar in TOC distribution, whereas the Ek_2^1 and Ek_2^2 have two high value zones, e.g., the Zaoyuan region and the Wangguantun-Xiaoji region, while the Ek_2^3 has only one high value zone in the Zaoyuan region (Figure 8a–c).
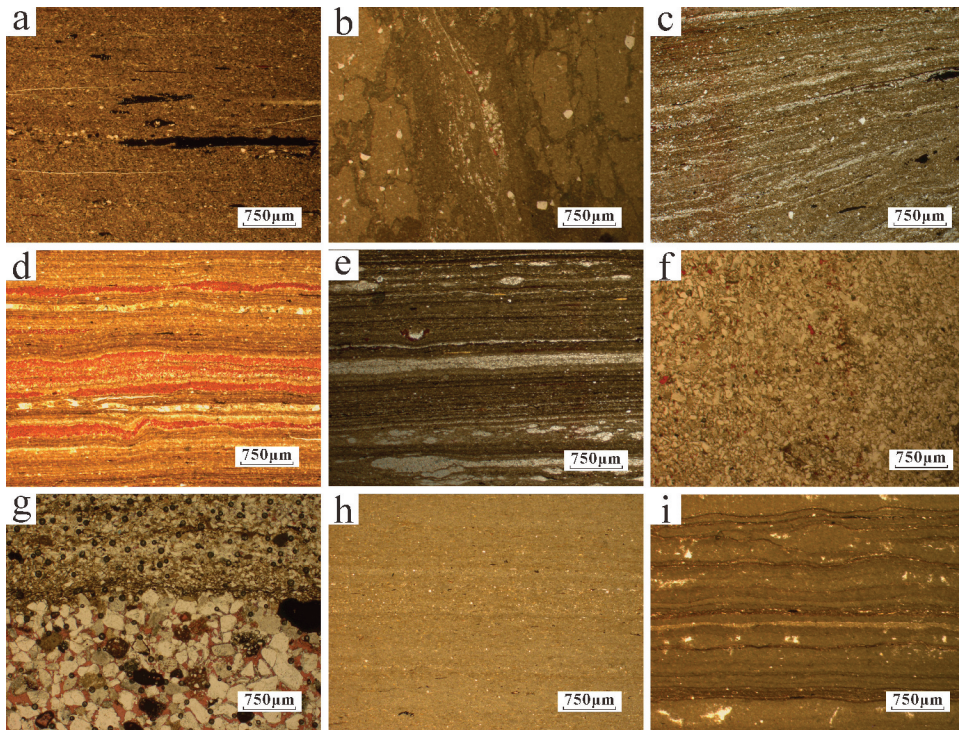
Figure 5. Thin-sections images showing different lithologies in the Ek_2: (a) F29-19, 2451.18 m, oil shale; (b) G89, 2866.23 m, mudstone; (c) G181, 2996.93 m, dolomitic shale; (d) F29-19, 2433.68 m, calcareous shale; (e) G995, 2917.07 m, silty shale; (f) G126, 3164.32 m, siltstone; (g) Z88, 2752.5 m, limestone-bearing silty lithic sandstone; (h) F29-19, 2447.32 m, dolomicrite; and (i) G33-56-1, 2492.08 m, argillaceous dolomite.

Extractible organic matter. The light hydrocarbons that had lost during sample storage and preparation had been added into the content of the chloroform bitumen "A" as per the research from Zhou et al. (2020). The chloroform bitumen "A" of the Ek_2^3 shale is in the range of 0.0045%–5.5787%, with an average value of 0.5883%, while the samples with the value of more than 0.2% account for 64.08%. The value of the Ek_2^2 shale ranges from 0.0011% to 5.9434% with an average value of 0.7236%, and the proportion of samples with the value of more than 0.2% is 73.63%. The value of the Ek_2^1 shale varies between 0.0033% and 1.9863%, with an average of 0.3033%, and the samples with the value of more than 0.2% account for 35.71% (Figure 7b). Generally, the average chloroform bitumen "A" of the Ek_2^2 and Ek_2^3 shales are higher than that of the Ek_2^1.

Hydrocarbon generation potential. The light hydrocarbons that had lost during sample storage and preparation and heavy hydrocarbon that was adsorbed in kerogen had been added into the content of the S_1 as per the research from Zhao et al. (2020). The hydrocarbon generation potential ($S_1+ S_2$) of the Ek_2^3 shale is 0.04–77.75 mgHC/gRock with an average of 22.99 mgHC/gRock, and the samples with the value more than 20 mgHC/gRock account for 47.2%. The $S_1+ S_2$ value of the Ek_2^2 shale is 0.07–58.86 mgHC/gRock with an average of 21.02 mgHC/gRock, while the samples with the value more than 20 mgHC/gRock account for 50.4%. The value of the Ek_2^1 shale is 0.03–34.34 mgHC/gRock with an average of 12.25 mgHC/gRock, and the samples with the value more than 20 mgHC/gRock account for 34.8%. Thus, the Ek_2^2 and Ek_2^3 shales have higher hydrocarbon generation potential than the Ek_2^1 (Figure 7c).

Table 1. Mineral compositions and clay mineral compositions of the Ek$_2$ shales in the Cangdong Sag.

Sample Number	Depth (m)	Strata	Mineral compositions (%)									Clay mineral compositions (%)						
			Qtz	Pot.	Pla.	Cal.	Dol.	Pyr.	Sid.	Ana.	Clay	I	K	C	I/S	C/S	Ratio of I/S	Ratio of C/S
F29-1	2435.29	Ek$_2^3$	10.6	0	1.2	0	81.2	0	0	0	7.0	-	-	-	-	-	-	-
F29-2	2447.32	Ek$_2^3$	4.4	0	3.8	0	82.6	0	0	1.9	7.3	9	1	2	88	0	45	0
F29-3	2433.68	Ek$_2^3$	27.2	0	7.2	8.0	0	0	0	1.9	55.7	-	-	-	-	-	-	-
F29-4	2451.18	Ek$_2^3$	24.3	0	6.4	13.2	0	5.4	0	2.3	48.4	-	-	-	-	-	-	-
F40-1	2435.59	Ek$_2^3$	22.7	0	10.1	0	0	0	6.2	1.8	59.2	-	-	-	-	-	-	-
F40-2	2442.32	Ek$_2^3$	53.3	13.6	19.6	0	0	0	0	0	13.5	9	3	3	85	0	30	0
F40-3	2449.46	Ek$_2^3$	35.9	4.6	16.2	9.3	0	0	0	8.4	25.6	15	3	4	78	0	30	0
F40-4	2460.73	Ek$_2^3$	21.1	0	6.9	0	0	3.5	0	1.3	67.2	9	2	2	87	0	50	0
G33-1	2485.23	Ek$_2^1$	10.3	0.8	1.9	14.2	37.7	0	0	15.1	20.0	-	-	-	-	-	-	-
G33-2	2492.08	Ek$_2^1$	8.6	0	2.6	0	75.6	0	0	10.0	3.2	-	-	-	-	-	-	-
G33-3	2490.47	Ek$_2^1$	19.1	5.7	4.4	15.7	23.6	0	0	18.4	13.1	21	5	6	68	0	30	0
G89-1	2866.23	Ek$_2^1$	9.7	0.7	4.8	6.4	0	0	0	24.0	54.4	10	5	10	60	15	25	40
G126-1	3164.32	Ek$_2^2$	46.8	7.5	27.2	9.3	0	0	0	0	9.2	34	20	46	0	0	0	0
G136-1	3194.90	Ek$_2^1$	14.3	0	9.6	21.9	25.9	0	0	14.5	13.8	8	4	12	31	45	25	45
G136-2	3197.71	Ek$_2^1$	16.4	6.0	9.9	4.7	11.0	2.8	0	28.5	20.7	-	-	-	-	-	-	-
G136-3	3298.81	Ek$_2^3$	19.0	0	19.1	10.8	26.9	0	0	10.7	13.5	-	-	-	-	-	-	-
G181-1	2996.93	Ek$_2^2$	8.1	0	2.4	0.4	60.1	0	0	18.9	10.1	-	-	-	-	-	-	-
G196-1	2847.09	Ek$_2^2$	16.1	0	6.5	2.8	22.3	0	0	32.2	20.1	15	2	4	75	4	15	40
G991-1	3558.46	Ek$_2^3$	47.4	4.3	18.1	12.9	0	0	0	0	17.3	6	7	31	56	0	55	0
G991-2	3562.94	Ek$_2^3$	24.6	0	6.0	14.7	0	0	0	0	54.7	11	4	9	76	0	30	0
G995-3	2917.07	Ek$_2^2$	10.6	4.4	5.2	4.9	0	20.9	3.7	25.1	25.2	9	3	4	84	0	20	0
G995-4	2916.81	Ek$_2^2$	11.9	1.4	8.4	0	26.2	0	0	27.6	24.5	-	-	-	-	-	-	-
G996-1	2931.89	Ek$_2^3$	44.6	6.4	32.7	5.9	0	0	0	0.9	9.5	12	4	8	76	0	35	0
G996-2	2936.29	Ek$_2^3$	20.0	0	8.6	13.0	2.7	0	0	10.7	45.0	8	2	2	88	0	45	0
G996-3	2932.62	Ek$_2^3$	42.8	4.6	19.1	5.1	0	1.3	0	5.6	21.5	9	3	9	79	0	30	0
G996-4	2944.45	Ek$_2^3$	7.0	0	1.7	0	77.5	0	0	3.8	10.0	-	-	-	-	-	-	-
J6-1	2570.92	Ek$_2^2$	22.9	3.9	16.5	8.8	0	0	0	27.7	20.2	17	1	5	55	22	15	40
J6-2	2572.51	Ek$_2^2$	16.5	1.3	9.7	8.7	6.8	0	0	30.3	26.7	16	0	3	69	12	15	35
Z88-1	2752.50	Ek$_2^3$	55.9	5.3	17.6	9.1	0	0	0	0	12.1	-	-	-	-	-	-	-

Qtz, Quartz; Pot., potassium; Pla., plagioclase; Cal., calcite; Dol., dolomite; Pyr., pyrite; Sid., siderite; Gyp., gypsum; Ana., analcime; S, smectite; I, illite; K, kaolinite; C, chloride; I/S, mixed illite and smectite; C/S, mixed chloride and smectite.
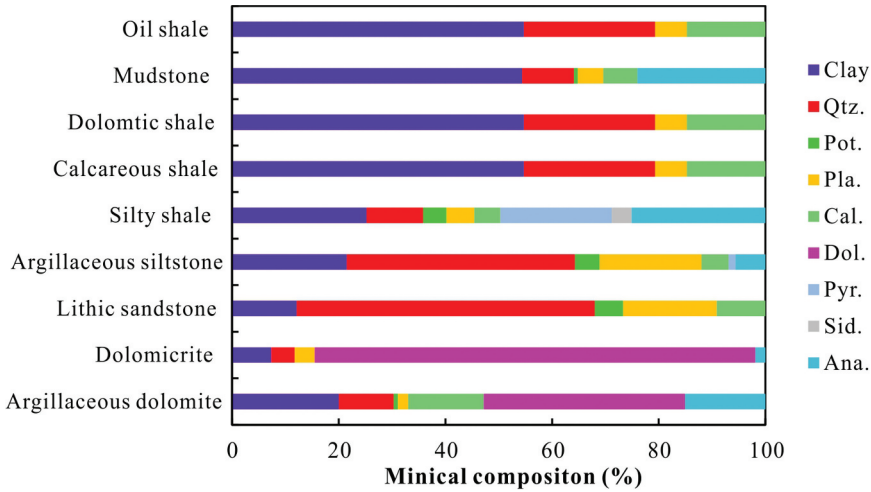
Figure 6. Mineral compositions of different lithologies in the Ek_2 system.

Table 2. Geochemical data of the Ek_2 shales in the Cangdong Sag from the study.

Sample Number	Depth (m)	Strata	TOC (%)	Ro (%)	S_1 (mg/g)	S_1 after correction (mg/g)	S_2 (mg/g)	Tmax (°C)	HI (mg/g)	PI
F29-1	2435.29	Ek_2^3	4.63	-	0.54	1.03	26.95	439	582	0.02
F29-2	2447.32	Ek_2^3	2.14	0.42	1.52	2.89	18.52	436	865	0.08
F29-3	2433.68	Ek_2^3	8.39	-	1.17	2.22	62.84	434	749	0.02
F29-4	2451.18	Ek_2^3	6.69	0.52	0.73	1.39	44.27	437	662	0.02
F29-5	2435.18	Ek_2^3	5.46	-	1.46	2.77	44.82	437	821	0.03
F40-1	2435.59	Ek_2^3	7.44	0.45	0.89	1.69	58.18	446	782	0.02
F40-4	2460.73	Ek_2^3	7.26	0.52	0.81	1.54	55.38	444	763	0.01
G33-1	2485.23	Ek_2^1	0.76	0.45	0.12	0.23	3.79	438	499	0.03
G33-3	2490.47	Ek_2^1	8.78	0.45	0.38	0.72	67.62	443	770	0.01
G89-1	2866.23	Ek_2^1	0.02	0.60	0.04	0.08	0.09	431	450	0.31
G136-1	3194.90	Ek_2^1	2.92	0.59	0.59	1.12	22.95	439	786	0.03
G136-2	3197.71	Ek_2^1	6.05	-	1.31	2.49	49.32	438	815	0.03
G136-3	3298.81	Ek_2^3	2.12	-	0.96	1.82	12.32	439	581	0.07
G181-1	2996.93	Ek_2^3	4.58	0.60	3.81	7.24	36.29	439	792	0.1
G181-2	2998.93	Ek_2^3	6.02	-	6.36	12.08	46.03	440	765	0.12
G196-1	2847.09	Ek_2^2	3.21	0.53	0.43	0.82	20.90	438	651	0.02
G991-2	3562.94	Ek_2^3	2.61	0.64	0.35	0.67	25.40	443	973	0.01
G995-1	2888.01	Ek_2^2	5.01	-	0.63	1.20	47.32	442	945	0.01
G995-2	2905.31	Ek_2^2	0.77	0.58	0.22	0.42	2.20	440	286	0.09
G995-3	2917.07	Ek_2^2	3.92	0.56	0.33	0.63	30.55	436	779	0.01
G995-4	2916.81	Ek_2^2	3.12	-	1.03	1.96	24.81	440	795	0.04
G996-2	2936.29	Ek_2^3	0.84	-	0.17	0.32	1.67	435	199	0.09
G996-4	2944.45	Ek_2^3	7.68	-	0.39	0.74	60.40	445	786	0.01
J6-2	2572.51	Ek_2^2	0.37	0.84	0.05	0.10	0.21	430	57	0.19
Z88-1	2752.50	Ek_2^3	6.33	0.59	13.45	25.56	36.46	431	576	0.27

PI = S1/(S1+ S2); HI = S2/TOC*100

Organic matter types

The HI-Tmax plots derived from the Rock-Eval pyrolysis results suggested that the Ek_2 shales mainly develop type I and II_1 organic matter with minor type II_2 and III organic matter (Figure 9). The organic matter types of different submembers show slight differences. The Ek_2^1 shale mostly develops type I and II_1 organic matter. Similarly, the Ek_2^2 shale develops abundant type I and II_1 organic matter and have a small number of type II_2 and III organic matter. The organic matter of Ek_2^3 shale is mainly type I.

Table 3. Geochemical data of the Ek_2 shales in the Cangdong Sag from the study and Dagang Oilfield.

Group	TOC (%)	"A" (%)	"A" after correction (%)	$S_1 + S_2$ (mg HC/ gRock)	HI (mg HC/ gRock)	Tmax (°C)
Ek_2^1	0.05–9.40	0.0019–1.1035	0.0033–1.9863	0.03–34.34	31–815	430–443
	2.69(76)	0.1685(42)	0.3033(42)	12.25(23)	530(10)	438(10)
Ek_2^2	0.08–7.43	0.0006–3.3019	0.0011–5.9434	0.07–58.86	17–945	427–449
	2.90(273)	0.4020(182)	0.7236(182)	21.02(115)	516(77)	438(77)
Ek_2^3	0.04–9.90	0.0025–3.0993	0.0045–5.5787	0.04–77.55	67–973	424–446
	3.44(135)	0.3268(103)	0.5883(103)	22.99(53)	637(35)	439(35)
Min-max avg. (number)						

Organic maturity

The Ro values of the Ek_2 organic-rich shale samples are 0.42%–0.84%, with most values less than 0.7%, which indicates most shales are in the stage of immature to low mature thermal evolution (Table 2). The Ro values of the Ek_2 shales are positively correlated with depth, which can be used to predict spatial variations of thermal maturity. Ro variations in the Ek_2^1, Ek_2^2 and Ek_2^3 shales were mapped using the empirical equation between measured Ro and the corresponding depth data. The thermal maturity of the Ek_2 shales in the Cangdong Sag is obviously controlled by the tectonic pattern. Immature to low maturity shales (Ro <0.7%) are mainly distributed in the central uplift (Kongdian Structural Belt) and the Nanpi slope in the southwest, while the Ro values in the Eastern Kongdian Slope and the Western Kongdian Slope are between 0.6% and 1.2% (Figure 10). Because the Ro value increases with depth, thermal maturity varies among different submembers in order: $Ek_2^3 > Ek_2^2 > Ek_2^1$ (Figure 10a–c).

Pore space characteristics and reservoir physical properties

Pore types and fractures from FE-SEM

FE-SEM images show various nano-micron scale pores in the Ek_2 shale, including intergranular pores, intragranular pores, dissolution pores, organic pores, and microfractures. The intergranular pores are generally narrow, elliptical, or irregular in shape with a width of hundreds of nanometers (Figure 11a), and commonly occurred among quartz, feldspar, and carbonate minerals. The intergranular pores of pyrite are sometimes filled with organic matter (Figure 11b). The dissolution pores commonly involve in dissolved feldspar grains and carbonate minerals, mostly with irregular enclosed outlines (Figure 11c). The organic pores are bubble-like or elliptical in shape with widths from tens to hundreds of nanometers. Additionally, some slit-shaped pores occurred at the edge of organic matter (Figure 11d). Microfractures are found locally, while some of them are filled by organic matter with a width of 130 nm (Figure 11c).

Pore structure characteristics based on N_2 adsorption

The N_2 adsorption and desorption curves and pore size distribution of the four Ek_2 shale samples present in Figure 12. The sample G33-1 is dolomite and has the highest adsorption volume, while the other samples are shales and have relatively low adsorption volume, which implies dolomite has higher pore volume than shales. All four samples develop hysteresis loops, and the shape of hysteresis loops are similar to a combination of type H_2 and type H_3 in the IUPAC classification (Figure 12a) (Sing 1985), which indicate that most pores in the Ek_2 samples are slit-like shape with openings at one or both ends and that ink-bottle-like pores are of secondary importance. The pore size distribution is characterized by a single peak at 3–5 nm (Figure 12b), which is different from the FE-SEM images (tens to hundreds of nanometers) due to the limited resolution of FE-SEM image observations (Nelson 2009).
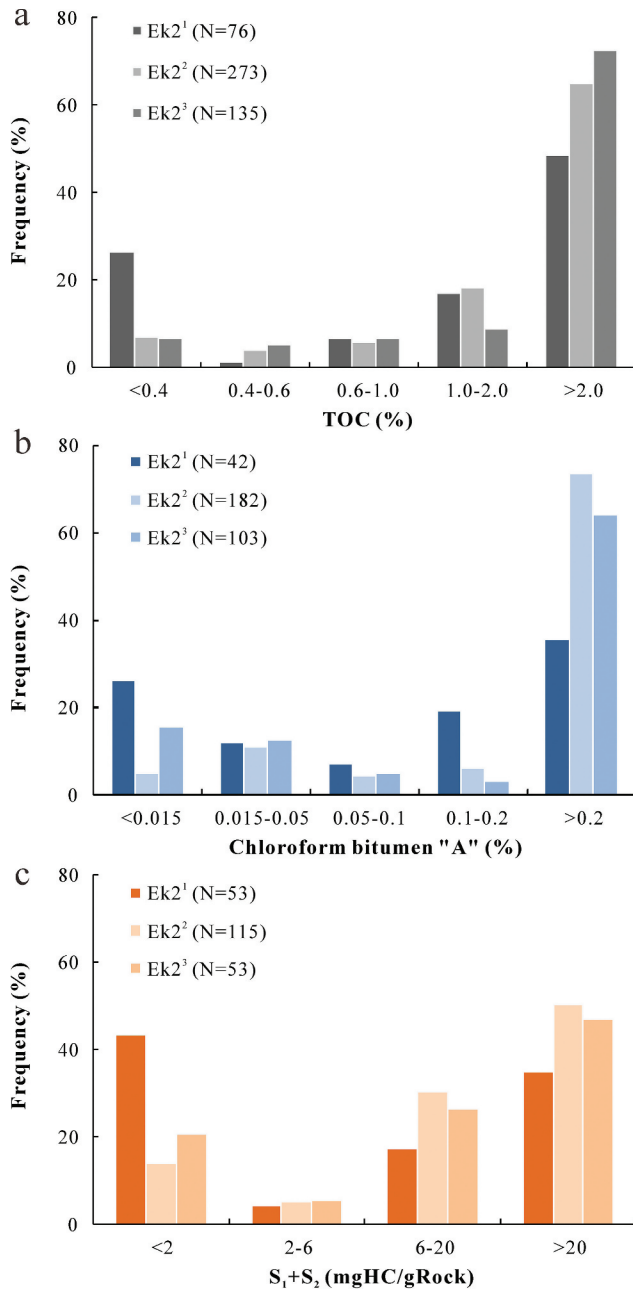
Figure 7. Histograms of organic matter abundance parameters: (a) TOC, (b) Chloroform bitumen "A", and (c) $S_1 + S_2$.

Physical properties of the Ek_2 reservoir

The physical property analyses of the Ek_2 shales show that porosity and permeability varied greatly among different lithologies (Figure 13). The porosity and permeability of shales are 0.57%–8.63% and $0.022–18.219 \times 10^{-3}$ μm^2, averaging 2.46% and 0.937×10^{-3} μm^2, respectively. The porosity and
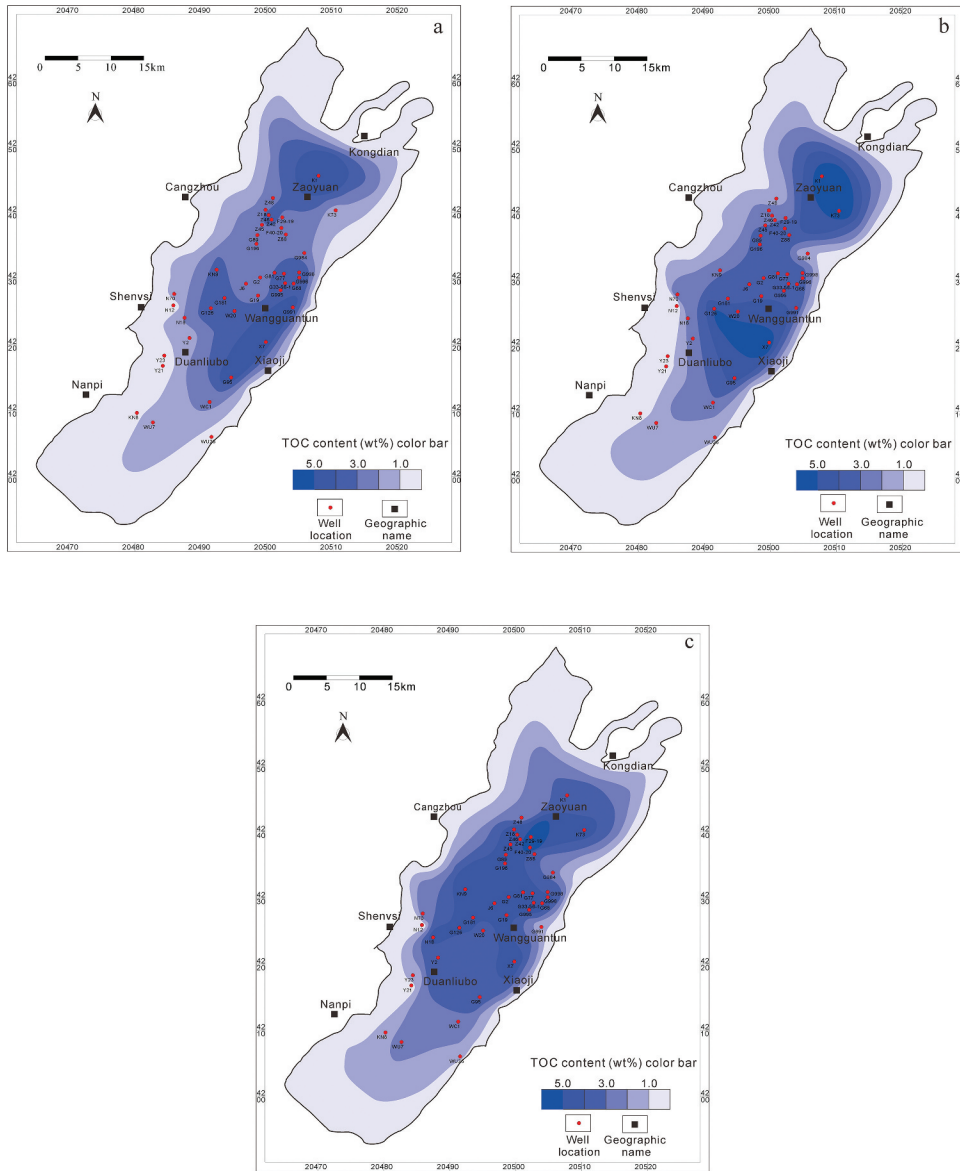
Figure 8. TOC distribution of (a) the Ek_2^1, (b) the Ek_2^2 and (c) the Ek_2^3.

permeability of interbedded dolomites are 0.47%–10.57% and 0.013–16.975 × 10^{-3} μm^2, averaging 5.26% and 1.910 × 10^{-3} μm^2, respectively. The values of interbedded sandstones are 5.20%–13.56% and 0.077–16.907 × 10^{-3} μm^2, averaging 8.66% and 2.207 × 10^{-3} μm^2, respectively (Zhao et al. 2017). The Ek_2 shale system has typically low porosity and low permeability, while the porosities and permeabilities are highest in sandstones, followed by dolomites, and are lowest in shales. In comparison, the reservoir quality of sandstones and dolomites are better than that of shales. Some shale samples possessing higher permeabilities are attributed to microfractures.
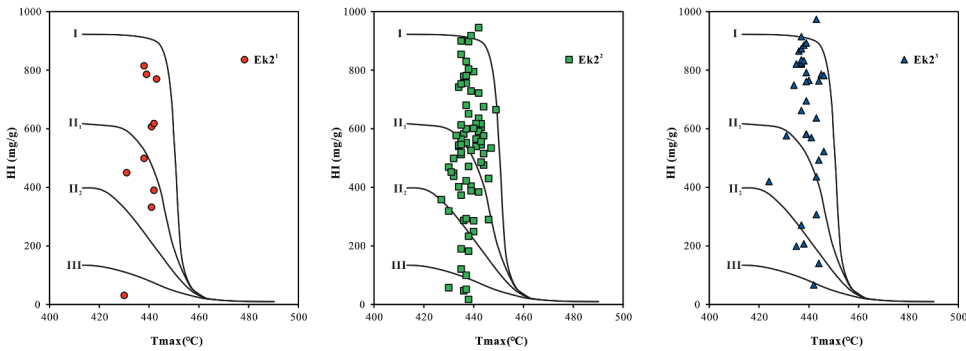
Figure 9. The organic matter types of the Ek_2 shale that identified by the HI-Tmax plots.

Discussion

Key factors that influence the Ek_2 shale oil system

Influence of lithology on the shale oil system

The Ek_2 shale system develops vertically frequent interbeds among mudstones, sandstones, and carbonate rocks, as shown in Figure 3. Different lithologies show different mineral compositions, physical properties, and various oil and gas shows, impacting the shale oil resources potential.

The mineral compositions of the Ek_2 shales are complex with no obvious predominant minerals. Previous studies have suggested that the Ek_2 shale system is dominated by fine-grained mixed rock facies (Yan et al. 2017). The brittle mineral content is high, with an average content of 73.86%, including quartz, feldspar, calcite, dolomite, pyrite, and zeolite, while clay mineral content is relatively low with an average of 26%. Britt and Schoeffler (2009) believe that clay mineral content in a favorable shale prospect play should be less than 40%. This mineral combination of the Ek_2 shale system is conducive to the fracture stimulation of shale reservoirs.

The occurrence of the liquid hydrocarbon in the shale system is heterogeneous, resulting in the local accumulation of shale oil. Taking some known shale oil system in North America, such as Bakken shale, Wolfcamp shale, Eagle Ford shale, etc., the main production layers of shale oil in the Bakken shale are dolomite, siltstone, and sandstone of the middle Bakken (Lillis 2013); the high-yielding layers of shale oil in the Wolfcamp shale are medium-thin conglomerate, granular marl, or marl in shale (Zhang et al. 2017); and the thin interlayer limestone in the Eagle Ford shale has the best liquid hydrocarbon production capacity (John et al. 2015). Thus, the carbonate rocks and sandstones in the shale system are prone to be the more favorable reservoir than the shales. The Ek_2 shales are sandwiched with a large number of sandstones and carbonate interlayers with better reservoir quality than that of shales, where liquid hydrocarbon is easier to extract. The hydrocarbon shows of the Ek_2 shale system from 154 wells in the Cangdong was statistically analyzed, suggesting that the oil saturation varies greatly with lithology in order: fine sandstone and siltstone > dolomite > shale (Figure 14).

Influence of pore structure on the shale oil system

FE-SEM images show that the nanoscale pores in the Ek_2 shale system are well developed with pore diameters of approximately dozens to hundreds of nanometers, which can be high-quality storage spaces for shale oil. The flowing of liquid hydrocarbon in the Ek_2 shale system is difficult without fractures considering that shale oil in-place is generally in terms of adsorbed oil and free oil (Li et al. 2017). Therefore, the existence of microfractures is of great significance to shale oil fluidity, and fracturing stimulation is important for the Ek_2 shale reservoirs.
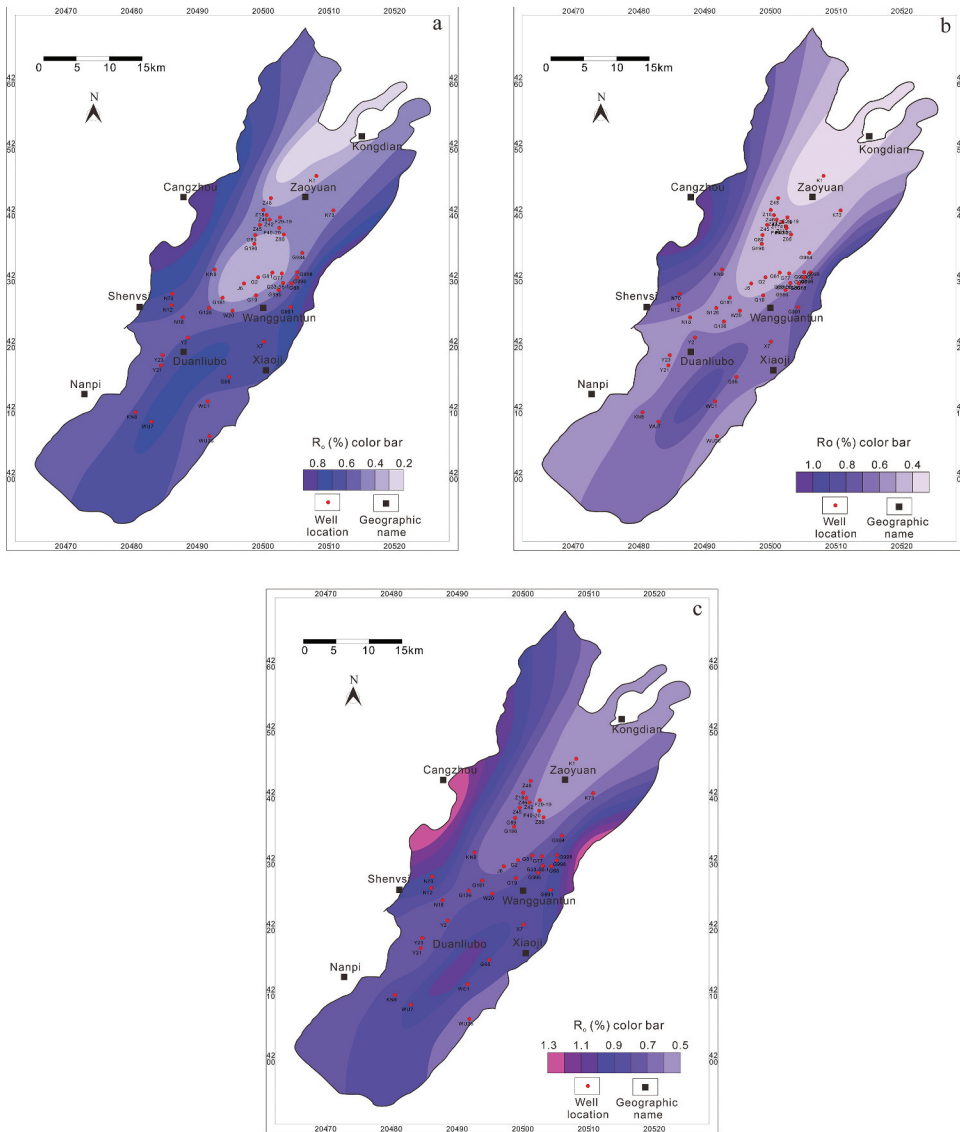
Figure 10. Vitrinite reflectance (Ro) spatial distributions of the Ek_2^1 (a), Ek_2^2 (b), Ek_2^3 (c) organic-rich shales.

The pore size of the Ek_2 shales derived from N_2 adsorption and desorption experiment ranges from 3 to 100 nm; and the pore size of intergranular pores, dissolution pores, organic pores in the FE-SEM images are about 50–800 nm. Those pores provide the storage space for the Ek_2 shale oil. Some microfracture with width of several hundred nanometers might be the effective migration pathway for shale oil.

Physical properties and oil-bearing properties vary with lithology, indicating obvious differences in oil and gas enrichment in shale systems, which is important for shale oil accumulation and "sweet spot" predictions. Comparatively, tight sandstone and dolomite interbeds have better reservoir physical properties and oil-bearing performances and thereby have better exploration potential for shale oil than the shale reservoir.
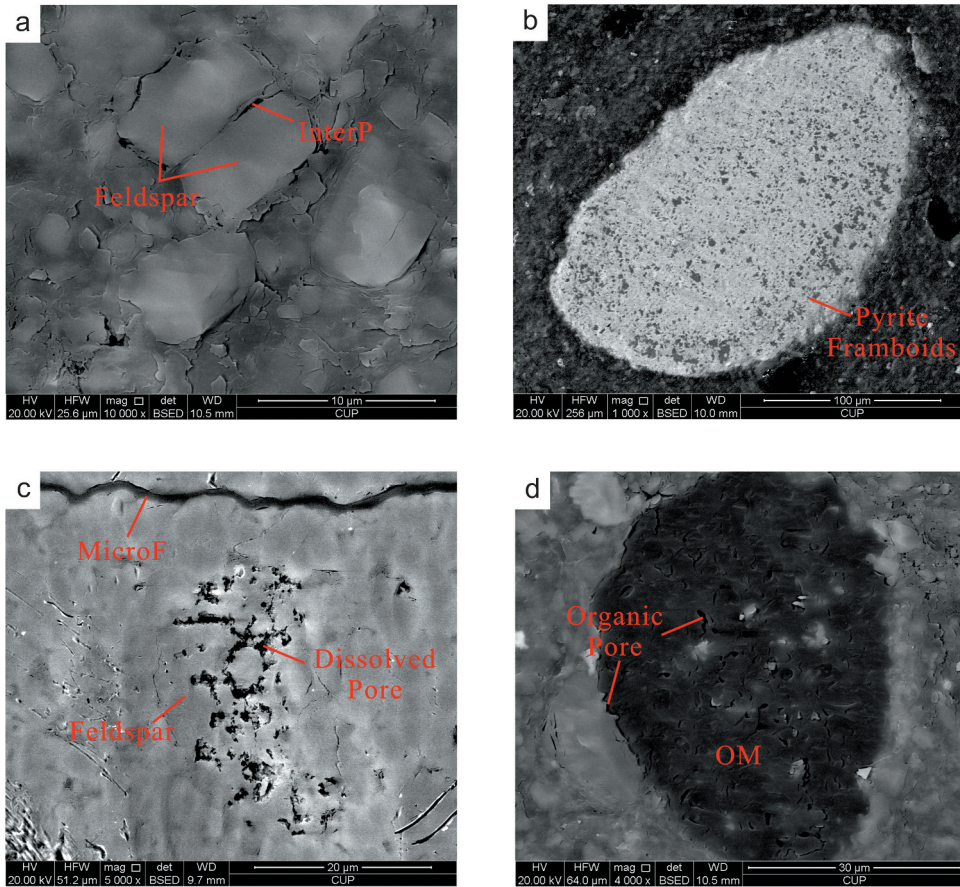
Figure 11. FE-SEM images of the Ek$_2$ shales in the Cangdong Sag: (a) G995, 2916.04 m, feldspar intergranular pore; (b) F40-20, 2460.73 m, intergranular pores in pyrite framboids; (c) F29-19, 2447.32 m, feldspar dissolution pores and microfracture; (d) F40-20, 2460.73 m, organic pores are regular-shaped, bubble-like or elliptical shape, width of 600–800 nm.
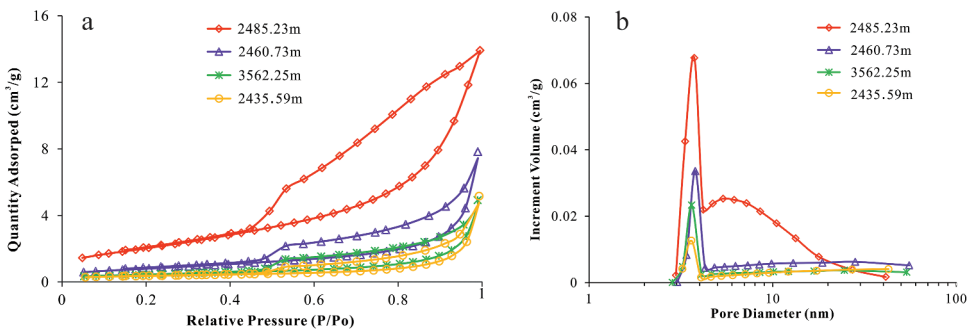

Figure 12. Low-pressure nitrogen gas adsorption and desorption curves of the Ek$_2$ shales. (a) Low-pressure nitrogen adsorption isotherms; (b) Pore size distributions.

Influence of geochemical properties on the shale oil system

The Rock-Eval parameter Tmax can be used to estimate the thermal maturity (Peters 1986; Yan and Song 2009). Wu (1986) summarized the relationship between Tmax and Ro of 60 source rocks from 55
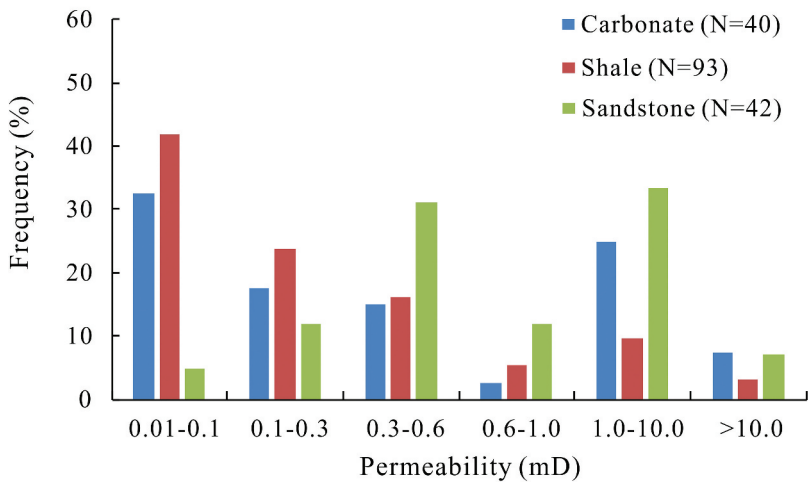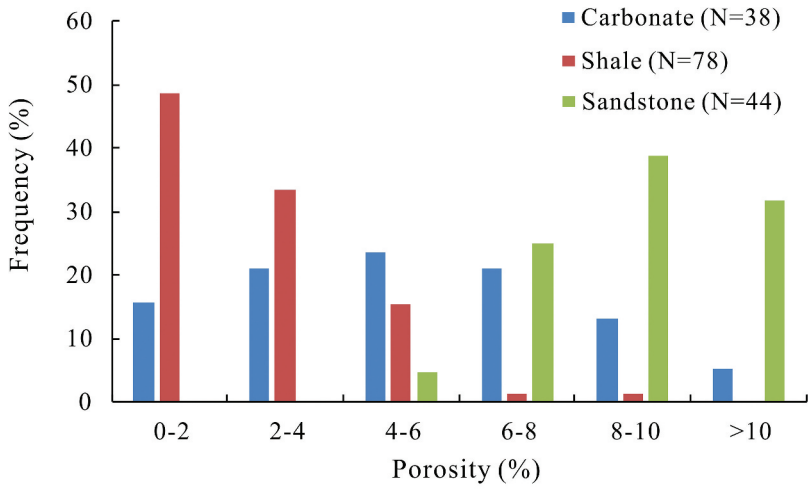
Figure 13. Porosity and permeability distribution of the Ek2 shale with different lithologies (The data were collected from Zhao et al. (2017)).
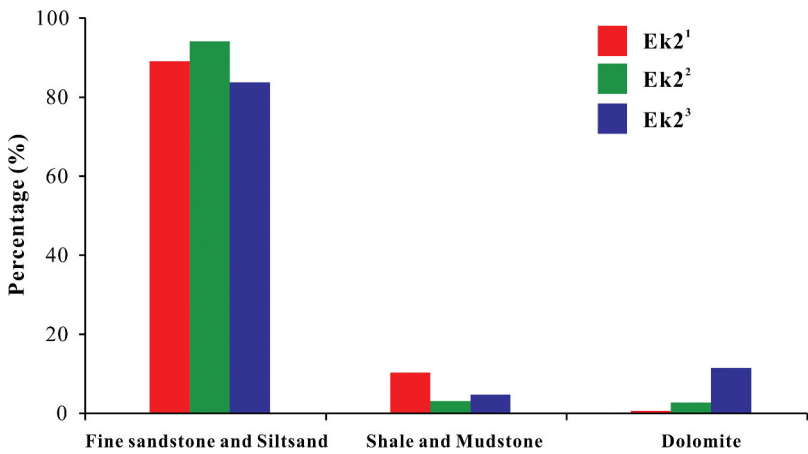

Figure 14. Oil-gas shows of different lithologies (sandstone, dolomite, shale) in the Ek$_2$ shale system.
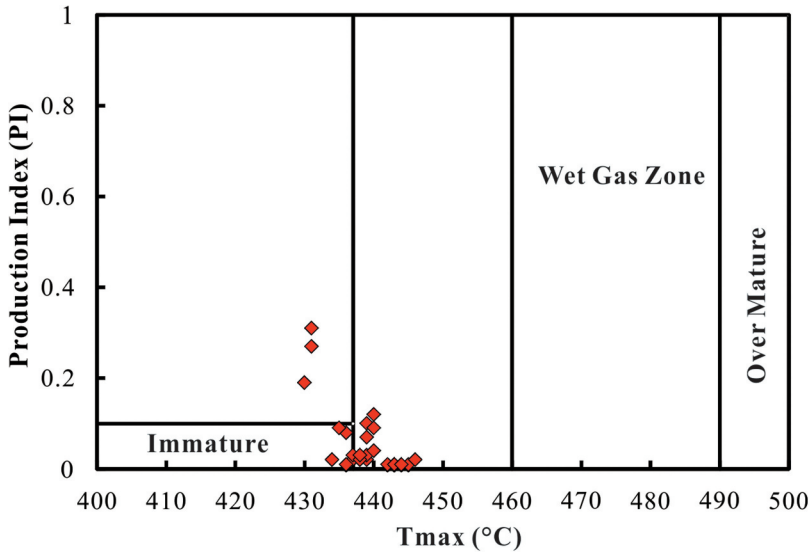
Figure 15. Plot of Tmax vs. PI showing the Ek_2 samples are immature to low mature.

regions in China and concluded that type I kerogen enters the oil generation threshold at 437°C of Tmax, began to generate wet gas at 460°C and dry gas at 490°C. The measured Tmax of the Ek_2 samples ranged from 430°C to 446°C, which suggests that they are immature and low mature shales (Figure 15). Most samples have low PI values ($PI = S_1/(S_1 + S_2)$) because of low maturity, but some immature samples show high PI values (Figure 16), which may be caused by migrated liquid hydrocarbon. A small number of samples with high oil saturation could be also identified from the TOC-S_1 cross plot, indicating the presence of migrating hydrocarbons (Figure 16) (Hui and Sonnenberg 2012; Peters 1986).
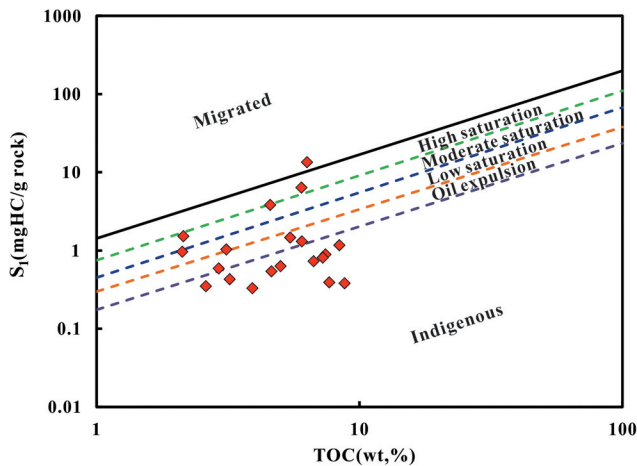

Figure 16. Plot of Tmax vs. S_1 suggesting a small portion of migrated hydrocarbon. Points above the black solid line represent migrated hydrocarbon, while points below the black solid line represent indigenous hydrocarbon. The boundary was determined from.Hui and Sonnenberg (2012)

These geochemical parameters indicate that the Ek_2 shales are characterized by high organic matter abundance with oil-prone kerogen, strong hydrocarbon generation capacity, and low maturity. Generally, the Ek_2 shale system has high shale oil resources potential with a small proportion of migrated hydrocarbon, which is a favorable member for shale oil enrichment.

Prediction for favorable areas of the shale oil system

The accumulation of the immature-low mature shale oil

The Tertiary "immature-low mature oil" in a rift basin in eastern China was generated by algae-rich soluble organic matter derived from saline and reductive deposition environments (Zhang 2008; Zhang et al. 1999). The Ek_2 shales in the Cangdong Sag, as a typical rift basin in eastern China, was traditionally regarded as the main source rocks in conventional oil and gas exploration. The hydrocarbon generation profile derived from actual geochemical data shows two hydrocarbon generation peaks, and immature oil was generated when Ro less than 0.5% (Liu, Liu, and Liu 2015). A physical simulation experiment suggested that the Ek_2 source rock began to generate and expel hydrocarbons at Ro <0.5%, and two oil generation peaks occurred at Ro of 0.5% and Ro of 0.9% (Figure 17) (Yang et al. 2007).

The liquid hydrocarbons in the shale system mainly occur as follows: 1) adsorbed oil on the surface of organic matter pores and mineral matrix pores with a certain pore size, and 2) free oil on various pores (Li et al. 2017; Wang et al. 2015). The former is controlled by several factors, e.g., pore or fracture width, thermal maturity, carbon chain length of alkanes, etc. (Wang et al. 2015). In terms of liquid hydrocarbons derived from the lacustrine immature to low mature shale, the intensive adsorption capacity is caused by longer carbon chains, higher viscosity and lower thermal maturity, obstructing the flow of liquid oil.
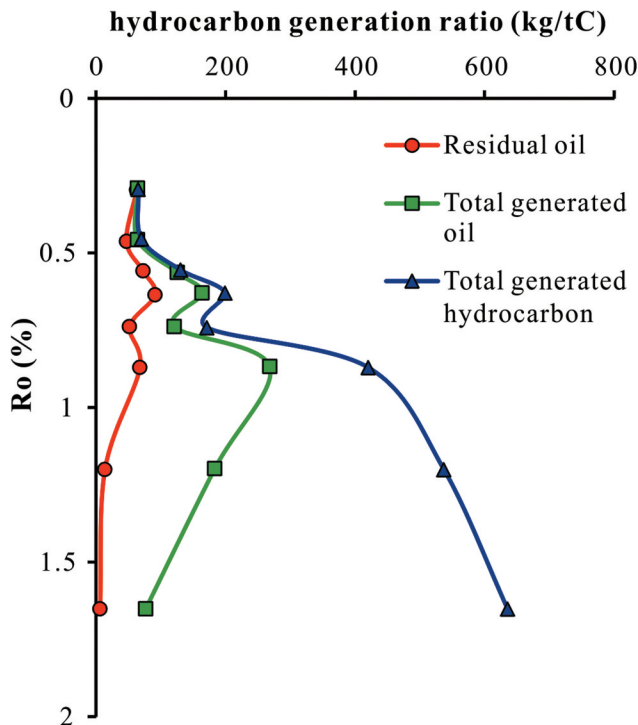

Figure 17. Hydrocarbon generation model of the Ek_2 shale (Yang et al. 2007).

The resources of the Ek_2 immature-low mature shale oil

Previous studies suggest that immature to low mature shales can generate considerable hydrocarbons, forming large-scale oil resources (Bao 2006; Wang et al. 1997). Lu et al. (2005) confirmed that the Ek_2 generated substantial immature to low mature liquid hydrocarbons. Zhou et al. (2017) used genetic methods, EUR analogy methods and small panel volumetric methods to calculate the Ek_2 shale oil resources in the Cangdong Sag. Finally, the Ek_2 in-place shale oil resources and recoverable resources in the study area were determined using the Delphi weighing method with values of 3.98×10^8 t and 0.58×10^8 t, respectively.

EUR is the ultimate recoverable reserve of a single well determined by production data, which can directly and effectively show recoverable reserves. Currently, only a few oil production wells are for the Ek_2 shale oil in the Cangdong Sag, for instance, the G68 and G107X1 wells have accumulated production for more than 3 years with well-controlled areas of 0.37 km^2 and EURs of 4.3×10^4 t and 1.9×10^4 t, respectively (Zhou et al. 2017). These EUR data are comparable to those in North America, e.g., the average shale oil EUR of Wolfcamp Shale in the Midland Basin is 2.63×10^4 t (Gaswirth et al. 2016), the EURs of the Middle Spraberry and Lower Spraberry are 2.05×10^4 t and 2.77×10^4 t, respectively (Marra et al. 2017), and the EUR of Bakken shale in the Williston Basin varies from 5.71×10^4 t in the Eastern Transitional to 2.33×10^4 t in the Northwest Transitional Continuous Oil (Cook 2013; Gaswirth and Marra 2015). The Ek_2 shale oil system has good shale oil production capacity and abundant oil resources, which indicates that the lacustrine immature to low mature shale oil has a bright exploration prospect.

Prediction for favorable areas

The Ek_2 shale reservoir profile was established based on lithology, oil and gas shows, log data and sequenced stratigraphic frameworks. As mentioned above, the Ek_2 shale system is predominated by mudstones, oil shales, sandstones, carbonate rocks, and a small amount of basalt. Sandstones and carbonate rocks interbeds in the Ek_2 shale system show better oil gas show and higher oil-saturated index (OSI, equivalent to $S_1/TOC*100$ (Jarvie 2012)) than shales (Figure 18), indicating sandstones
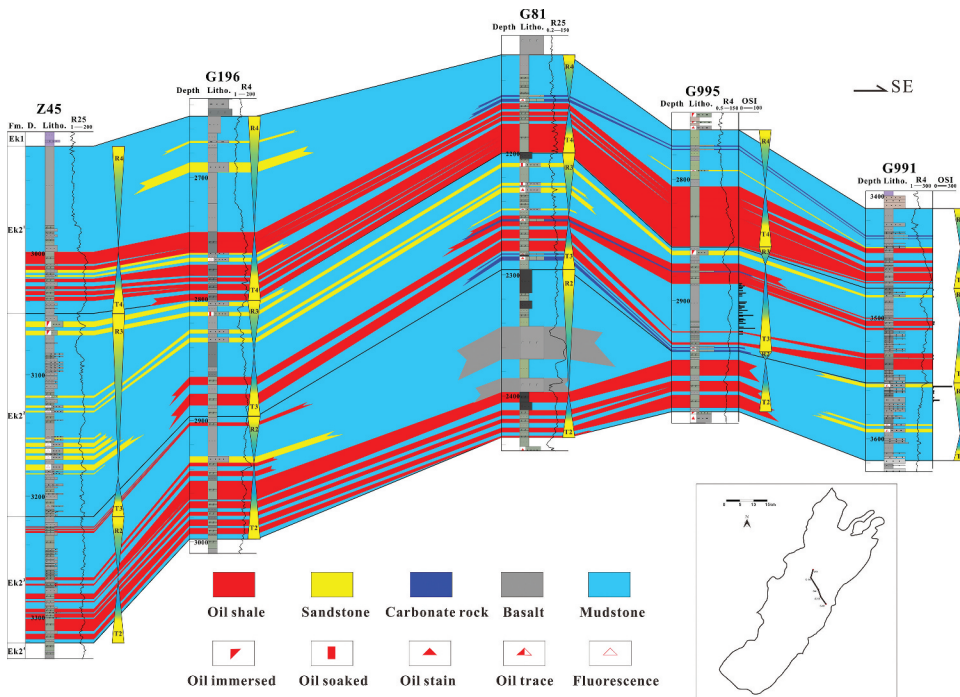

Figure 18. Vertical variation of the lithology in the Ek_2 shale system.

and carbonate rocks interbeds possess greater shale oil potential. In addition, organic maturity plays an important role in shale oil fluidity (Han et al. 2017), the mobility of shale oil increases obviously when the Ro values are more than 0.7% (Lu et al. 2012). The area with Ro more than 0.7% should take precedence over other areas, which means the slope zones are more favorable than Kongdian Structure Belt laterally and the Ek_2^3 and Ek_2^2 are more potential for shale oil accumulation than the Ek_2^1 vertically (Figure 10). By identifying and tracing these fine siltstone and carbonate interlayers with good oil and gas shows and integrating with organic maturity, we can effectively seek shale oil enrichment zones and facilitate the deployment of horizontal wells.

Conclusions

The geological characteristics and shale oil resource potential of the Ek2 shale were investigated in this study. The following conclusions were drawn:

(1) The Ek_2 organic-rich shale system is well developed in the Cangdong Sag, Huanghua Depression, Bohai Bay Basin, with a maximum thickness of 600 m. The Ek_2^1, Ek_2^2 and Ek_2^3 are mainly deposited in semi-deep to deep lakes, forming a large set of shale successions with thin sandstone and carbonate sandwiches. The Ek_2 shale system is predominated by shales, sandstones and dolomites, which can be subdivided into various mixed lithologies. The mineral compositions of the Ek_2 shales are complex with no obvious predominant minerals. The brittle mineral content is high with an average content of 73.86%, which is conducive to reservoir stimulation.

(2) The Cenozoic lacustrine Ek_2 shales are characterized by an abundance of high organic matter, oil-prone kerogens, large hydrocarbon generating potential, and low thermal maturity. Abundant immature to low mature liquid hydrocarbons have been generated, most of which remain in the shale system, while some migrated to adjacent continental clastic reservoirs. The in-place shale oil resources are 3.98×10^8 t, and the recoverable resources are 0.58×10^8 t. The EUR of Ek_2 shale oil system can be comparable to that of the typical North America shale oil systems.

(3) The Ek_2 shales develop various pore types, including intergranular pores, intragranular pores, dissolution pores, organic pores, and microfractures. Nano-micron scale pores are well developed with pore diameters of approximately dozens to hundreds of nanometers, which provides storage space for shale oil. Microfracture plays a key role in the migration of shale oil.

(4) Different lithologies show different mineral compositions, physical properties, and various oil and gas shows. Physical properties of sandstones and dolomites are obviously better than shales. Sandstones and dolomites also have better oil and gas shows than shales. All of the above indicate that sandstones and carbonate interbeds in the shale system have better exploration potential. The area with Ro more than 0.7% should take precedence over other areas in light of the impact of organic maturity on shale fluidity. The slope zones are more favorable than Kongdian Structure Belt laterally and the Ek_2^3 and Ek_2^2 are more potential for shale oil accumulation than the Ek_2^1 vertically. This study demonstrates the immense resources potential of lacustrine shales, the engineering characteristics will be taken into account for locating the integrated sweet spots in the future.

Funding

Notes on contributors

Xiaoping Liu received his Ph.D. from China University of Petroleum-Beijing in 2002. He now is an associate professor at the college of Geosciences of the China University of Petroleum-Beijing and supervises graduate students. His technical specialties and current research interests include petroleum accumulation and geological evaluation of shale reservoir.

Ming Guan graduated in 2017 with an M.S. degree in Geological Resources and Geological Engineering and is now a Ph. D. student at the China University of Petroleum–Beijing. His current research interest is geological evaluation of shale reservoir.

Zhijun Jin is a Member of Chinese Academy of Sciences. He is Professor of Institute of Energy, Peking University and is also the Director of State Key Laboratory of Shale Oil and Gas Enrichment Mechanisms and Effective Development. He has long been engaged in research on petroleum geology and energy strategy.

Jin Lai is now a lecturer teaching reservoir geology and well logging geology in the College of Geosciences at the China University of Petroleum–Beijing. His current research interests include sedimentology, diagenesis, reservoir geology, pore structure, and well log analysis. He has also worked extensively with numerous types of unconventional reservoirs, including tight gas sandstones and tight oil plays in Ordos basin, Sichuan basin, and Tarim basin, China.

Shanyong Chen is a senior engineer at PetroChina Dagang Oil Field Company. His research interest mainly engages in Formation and distribution of oil and gas reservoirs.

ORCID

Ming Guan 🆔 http://orcid.org/0000-0002-0190-260X

References

Bao, J. 2006. Geochemistry of immature-low mature oil in Salt Lake Basin. *Geological Publishing House* 1–194.

Barrett, E. P., L. G. Joyner, and P. P. Halenda. 1951. The determination of pore volume and area distributions in porous substances. I. Computations from nitrogen isotherms. *Journal of the American Chemical Society* 73 (1):373–80.

Britt, L. K., and J. Schoeffler. 2009. *The geomechanics of a shale play: What makes a shale prospective*. West Virginia, USA: SPE Eastern Regional Meeting.

Cook, T. A. 2013. Procedure for calculating estimated ultimate recoveries of Bakken and Three Forks Formations horizontal wells in the Williston Basin. *Open-File Report*.

Deng, Y., S. Chen, X. Pu, and J. Yan. 2020. Characteristics and controlling factors of shale oil reservoir spaces in the Bohai Bay Basin. *Acta Geologica Sinica-English Edition* 94 (2):253–68. doi:10.1111/1755-6724.14286.

Donovan, A., J. Evenick, L. Banfield, N. Mclnnis, and W. Hill. 2017. An organofacies-based mudstone classification for unconventional tight rock and source rock plays. In: SPE/AAPG/SEG, Unconventional resources technology conference, Austin.

Gaswirth, S. B., and K. R. Marra. 2015. U.S. geological survey 2013 assessment of undiscovered resources in the Bakken and Three Forks Formations of the U.S. Williston Basin Province. *AAPG Bulletin* 99 (4):639–60. doi:10.1306/08131414051.

Gaswirth, S. B., K. R. Marra, P. G. Lillis, T. J. Mercier, and H. M. Leathers-Miller. 2016. Assessment of undiscovered continuous oil resources in the Wolfcamp shale of the Midland Basin, Permian Basin province, Texas. *United States Geological Survey* 1–4.

Han, Y., B. Horsfield, R. Wirth, N. Mahlstedt, and S. Bernard. 2017. Oil retention and porosity evolution in organic-rich shales. *AAPG Bulletin* 101 (6):807–27. doi:10.1306/09221616069.

Huang, D., and J. Li. 1987. Immature petroleum in continental deposits and its significance. *Acta Petrolei Sinica* 8 (1):1–9.

Hui, J., and S. A. Sonnenberg. 2012. Source rock potential of the Bakken shales in the Williston Basin, North Dakota and Montana. In: *American Association of Petroleum Geologists Annual Convention and Exhibition*, California, USA.

Jarvie, D. M. 2012. Shale resource systems for oil and gas: Part 2 - Shale oil resources systems. In *Shale reservoirs*, ed. J. A. Breyer., Vol. 97, pp. 89–119. Memoir: AAPG.

John, B., R. H. Wilty, Y. Tian, A. Salman, K. W. O'Connor, B. Kurtoglu, R. J. Hooper, R. M. Daniels, R. W. Butler, and D. Alfred. 2015. Limestone frequency and well performance, Eagle Ford shale (Cretaceous), South Texas. In Geoscience Technology Workshops, Fourth Annual Eagle Ford Shale, San Antonio, Texas.

Katz, B., and F. Lin. 2014. Lacustrine basin unconventional resource plays: Key differences. *Marine and Petroleum Geology* 56:255–65. doi:10.1016/j.marpetgeo.2014.02.013.

Li, J. Q., S. F. Lu, L. Xie, J. Zhang, H. T. Xue, P. Zhang, and S. S. Tian. 2017. Modeling of hydrocarbon adsorption on continental oil shale: A case study on n-alkane. *Fuel* 206:603–13. doi:10.1016/j.fuel.2017.06.017.

Lillis, P. G. 2013. Review of oil families and their petroleum systems of the Williston Basin. *Mountain Geologist* 50 (1):5–31.

Liu, X. P., Q. Liu, J. Liu, Q. Y. Dong, M. Guan, and H. X. Li. 2015. Geochemical characteristics of organic-rich shales of the second member of Kongdian Formation in Cangdong Sag, Huanghua Depression. *Lithologic Reservoirs* 27 (6):15–22.

Lu, S., C. Guo, J. Shen, and F. Wang. 2005. Application of chemical kinetic theory in resource evaluation of immature to low-mature oil in Huanghua Depression. *China Petroleum Exploration* 19 (6):18–23+90.

Lu, S. F., W. B. Huang, F. W. Cheng, J. J. Li, M. Wang, H. T. Xue, W. M. Wang, and X. Y. Cai. 2012. Classification and evaluation criteria of shale oil and gas resources: Discussion and application. *Petroleum Exploration and Development* 39 (2):249–56. doi:10.1016/S1876-3804(12)60042-1.

Marra, K. R., S. B. Gaswirth, C. J. Schenk, and H. M. Leathers-Miller. 2017. Assessment of undiscovered oil and gas resources in the Spraberry Formation of the Midland Basin, Permian Basin province, Texas. *United States Geological Survey* 1–2.

Nelson, P. H. 2009. Pore-throat sizes in sandstones, tight sandstones, and shales. *AAPG Bulletin* 93 (3):329–40. doi:10.1306/10240808059.

Passey, Q. R., S. Creaney, J. B. Kulla, F. J. Moretti, and J. D. Stroud. 1990. A practical model for organic richness from porosity and resistivity logs. *AAPG Bulletin* 12 (74):1777–94.

Peng, H. Y., J. Z. Liu, Y. Li, D. Q. Xiao, Z. C. Liu, S. Q. Yuan, X. G. Pu, D. Z. Qiu, B. Han, Y. P. Lan, et al. 2010. Study on continental sequence strata framework and oil and gas exploration: A case study of the Kongdian Formation in Kongnan area, Huanghua Depression. *Geophysical Prospecting for Petroleum* 49 (3):287–94. +6.

Peters, K. E. 1986. Guidelines for evaluating petroleum source rock using programmed pyrolysis. *AAPG Bulletin* 70 (3):318–29.

Pu, X. G., L. H. Zhou, W. Han, J. Zhou, W. Wang, W. Zhang, S. Y. Chen, Z. N. Shi, and S. Liu. 2016. Geologic features of fine-grained facies sedimentation and tight oil exploration: A case from the second Member of Paleogene Kongdian Formation of Cangdong sag, Bohai Bay Basin. *Petroleum Exploration and Development* 43 (1):24–33. doi:10.1016/S1876-3804(16)30003-9.

Sarı, A., M. A. Vosoughi, and P. Akkaya. 2015. Evaluation of source rock potential, matrix effect and applicability of gas oil ratio potential factor in Paleocene–Eocene bituminous shales of Çamalan Formation, Nallıhan-Turkey. *Marine Petroleum Geology* 67:180–86. doi:10.1016/j.marpetgeo.2015.05.020.

Sing, K. S. W. 1985. Reporting physisorption data for gas/solid systems with special reference to the determination of surface area and porosity (Recommendations 1984). *Pure & Applied Chemistry* 57 (4):603–19. doi:10.1351/pac198557040603.

Talbot, M. R. 1988. The origins of lacustrine oil source rocks: Evidence from the lakes of tropical Africa. *Geological Society* 40 (6):29–43. doi:10.1144/GSL.SP.1988.040.01.04.

Tissot, B. P. 1987. Thermal history of sedimentary basins, maturation indices, and kinetics of oil and gas generation. *AAPG Bulletin* 71 (12):1445–66.

Wang, S., Q. H. Feng, F. Javadpour, T. Xia, and Z. Li. 2015. Oil adsorption in shale nanopores and its effect on recoverable oil-in-place. *International Journal of Coal Geology* 147-148:9–24. doi:10.1016/j.coal.2015.06.002.

Wang, T., N. N. Zhong, D. Hou, G. Huang, J. Bao, and X. Li. 1995. *Formation mechanism and distribution of low mature oil and gas*. Beijing: Petroleum Industry Press.

Wang, T. G., N. N. Zhong, D. J. Hou, J. Bao, G. Huang, and X. Li. 1997. Several genesis mechanisms of low maturity oil in China. *Acta Sedimentogica Sinica* 15 (2):75–83.

Wang, Z. Y., Y. Z. Wei, and C. Y. Zhao. 2001. The immature oils in Santanghu Basin. *Acta Sedimentologica. Sinica* 19 (4):598–604.

Wu, L. 1986. *Quick quantitative evaluation of source rock pyrolysis*. Beijing: Science Press.

Yan, F., and Y. Song. 2009. Investigation of factors influencing the pyrolysis process for Fushun oil shale. *Energy Sources, Part A: Recovery, Utilization, and Environmental Effects* 31 (5):406–11.

Yan, J. H., Y. Deng, X. G. Pu, L. H. Zhou, S. Y. Chen, and Y. X. Jiao. 2017. Characteristics and controlling factors of fine-grained mixed sedimentary rocks from the 2nd Member of Kongdian Formation in the Cangdong Sag, Bohai Bay Basin. *Oil & Gas Geology* 38 (1):98–109.

Yang, G. F., D. L. Wang, M. Zhang, and X. M. Yu. 2007. Simulation experiment of hydrocarbon generation and expulsion of source rocks of Kongnan area in Dagang Oilfield. *Journal of Oil and Gas Technology* 29 (3):214–16. +511.

Ye, L., J. X. Zhang, G. C. Lu, and Z. Y. Zhang. 2013. Paleogene structure-stratigraphic framework and multiple episode evolution in Kongdian area, Huanghua Depression. *Earth Science-Journal of China University of Geosciences* 38 (2):379–89.

Zhang, H., X. Janson, L. Liu, and Z. Wang. 2017. Lithofacies, diagenesis, and reservoir quality evaluation of Wolfcamp unconventional succession in the Midland Basin, West Texas. In: *AAPG 2017 Annual Convention and Exhibition*, Houston, Texas, United States.

Zhang, L., S. Zhang, K. Huang, Q. Zhuo, Z. Hong, D. Huang, and T. Wang. 1999. Simulated experimental study on genesis mechanism of immature oil in brackish lake facies. *Chinese Science Bulletin* 44 (4):361–67.

Zhang, L. Y. 2008. The progress on the study of lacustrine source rocks. *Petroleum Geology & Experiment* 30 (6):591–95.

Zhao, X. Z., L. H. Zhou, X. G. Pu, F. Jin, W. Han, D. Xiao, S. Chen, Z. Shi, W. Zhang, and F. Yang. 2018. Geological characteristics of shale rock system and shale oil exploration in a lacustrine basin: A case study from the Paleogene 1st sub-member of Kong 2 Member in Cangdong sag, Bohai Bay Basin, China. *Petroleum Exploration and Development* 45 (3):361–72. doi:10.1016/S1876-3804(18)30043-0.

Zhao, X. Z., L. H. Zhou, X. G. Pu, W. Han, F. Jin, D. Xiao, Z. Shi, Y. Deng, W. Zhang, and W. Jiang. 2019. Exploration breakthroughs and geological characteristics of continental shale oil: A case study of the Kongdian Formation in the Cangdong Sag, China. *Marine and Petroleum Geology* 102:544–56. doi:10.1016/j.marpetgeo.2018.12.020.

Zhao, X. Z., X. G. Pu, L. H. Zhou, F. M. Jin, Z. N. Shi, W. Z. Han, W. Y. Jiang, and W. Zhang. 2020. Typical geological characteristics and exploration practices of lacustrine shale oil: A case study of the Kong-2 member strata of the Cangdong Sag in the Bohai Bay Basin. *Marine and Petroleum Geology* 113:1–14.

Zhao, X. Z., X. G. Pu, W. Han, L. H. Zhou, Z. N. Shi, S. Y. Chen, and D. Q. Xiao. 2017. A new method for lithology identification of fine grain deposits and reservoir sweet spot analysis: A case study of Kong2 Member in Cangdong sag, Bohai Bay Basin, China. *Petroleum Exploration and Development* 44 (4):492–502.

Zhou, F., D. Peng, L. Bian, D. Huang, and Y. Wang. 2002. Progress in the organic matter study of immature oils in the Qaidam Basin. *Acta Geologica. Sinica* 76 (1):107–13.

Zhou, L. H., C. Yu, S. Hua, C. Sun, and N. Wang. 2017. Shale oil resource estimation and application in Kong2 Member of Cangdong Sag. *Special Oil & Gas Reservoir* 24 (6):1–6.